Post-fire erosion potential of clayey sand soils and slopes – A laboratory study

Tabassum T¹., Lingwall B.N²., Bheemasetti T.V³., and Ferris, A.⁴

¹Ph.D. Student, Department of Civil and Environmental Engineering, South Dakota School of Mines and Technology, Rapid City, South Dakota 57701; e-mail: tanzila.tabassum@mines.sdsmt.edu

²Associate Professor, Department of Civil and Environmental Engineering, South Dakota School of Mines and Technology, Rapid City, South Dakota 57701; e-mail: bret.lingwall@sdsmt.edu
³Assistant Professor, Department of Civil and Environmental Engineering, South Dakota School of Mines and Technology, Rapid City, South Dakota 57701; e-mail: tejo.bheemasetti@sdsmt.edu
⁴Graduate Student, Department of Civil and Environmental Engineering, South Dakota School of Mines and Technology, Rapid City, South Dakota 57701; e-mail: andrew.ferris@mines.sdsmt.edu

Abstract: One of the principal side effects of wildland fire extreme events is mass soil erosion event of the soil and slopes denuded by the fire. These soil erosion events may be devastating and extreme in their own rights, damaging critical infrastructure downslope or downstream of the fire burn scars. While there are many variables influencing the severity of post fire erosion, the amounts of soil erosion are largely dependent on the water content of the soil at the time of the fire coupled with the fire intensity. Fires that are lower intensity or soils that are "wet" at time of burning have significantly less damage to root structures of grasses and other plants while showing lessened soil erosion potential. Fires that are higher intensity or on dry soils have higher damages to root structures and increased soil erosion potential. In this laboratory study, a single clayey sand soil material common to the ground surface across the Black Hills of South Dakota and Wyoming is studied for erosion potential after burning in a controlled container burn. This material is varied by initial water content and burned at a soil surface temperature of 800 Celsius for 75 minutes, a temperature-time continuum consistent with severe wildland fire. Burning is used rather than kilns to preserve the same atmospheric conditions as in the field fire event. A laboratory soil-erosion device is then used to measure soil erosion potential across a range of fluid velocities and soil slopes. The results of this study show that the initial water content of the soil at the time of fire is a key parameter in understanding soil erosion potential post-fire. While not a complete study on time-temperature-water content across many soil types, this pilot research shows promise for future models and mapping tools. These future tools will enable planners to target resources for post wildfire erosion mitigation based on surficial soil water content at the time of the fire.

Keywords: Soil Erosion, Fine-Grained Soil, Wildfire

1. Introduction

Working in the areas of geography and natural resources, DeBano, Doer, Robichaud and their colleagues extensively studied soil erosion after wildland fire from a largely empirical perspective, examining mass loss rates after rain and snow events that followed intense and severe wildland fires in both North America and Australia (DeBano 2000a and 2000b, Doer et al., 2000, and Robichaud 2000). Their work showed that soil erosion after wildland fire is a complex phenomena that is subject to a host of variables including, burn severity and duration, soil heat transfer, water content at the time of burning, surficial fuel loading in the duff, humus content, soil type,

mineralogy, organic content chemical composition, weather, precipitation event, time after burning, and ground slope (Robichaud 2002). Due to the exhausting requirements to study each variable in isolation, field observations and empiricism have been largely employed in the past to study post-fire soil erosion. However, if engineers are to aid in the post-fire remediation and rehabilitation of ground denuded by fire, additional studies into the mechanisms and propensities of erosion of these burned soils are warranted.

Soil erosion involves separation of soil particles due to the stresses induced by wind or water. In scour type erosion processes, an increase in the fluid velocity of water or wind results in an increase in the shear stresses acting on soil particles. When the applied shear stress from the moving fluid overcomes the particle bond strength and/or the weight of the particle, soil particles glide over each other causing erosion (Briaud et al., 2001). Alternative erosion pathways to scour type also occur, examples include high-water erosion, wave induced erosion, and internal piping erosion within earth structures (Bryan, 2000). For the purposes of this paper, we focus on wind and water erosion of the scour type only, with emphasis on water erosion.

In general terms, less compacted soils with high porosity are more prone to separation of loose soil particles due to fluid movements and are thus more erodible (Liu et al. 2012). Soils with less internal cohesion are likewise known to be more erodible. Many researchers have studied the correlation between soil properties and soil erodibility (Wischmeier and Mannering, 1969; Le Bissonnais et al., 1995; Dong-Sheng et al., 2006; Bonilla and Johnson, 2012). Earlier studies by Shields (1936) illustrated that the critical shear stress (shear stress at which soil erosion is initiated) of cohesionless soil is proportional to D₅₀ (mean diameter of the soil particle size distribution). For cohesive soils, Grissinger (1966) presented the relation between the plasticity of fine-grained soil with its erodibility, where high plastic soils have low erodibility and low plastic soils have higher degree of erodibility. However, the erodibility of fine-grained soils is complicated by internal matric suction such that the critical shear stress increases as the soil dries below plastic limit and decreases as the moisture increases above plastic limit (Al-Durrah and Bradford, 1982; Singh and Thompson, 2016).

While the principles of conventional surface erosion of soils hold for the burned paradigm after wildland fire, additional considerations must be made for the alterations in the soils composition, texture, and chemistry from the fire event itself. Foremost of these is soil hydrophobicity, which repels water from discrete layers in the soil where chemical changes to the soil have changed the naturally hydrophilic soil grains to be hydrophobic (Robichaud et al., 1999, 2000a and 2000b). To initiate an in-depth and robust study of soil erosion after wildland fire, this research presented in this paper provides initial pilot data to better guide the engineering researcher who is interested or has cause to study the remediation of mass soil erosion events in the wildfire environment.

It is necessary to interpret the test results based on the recorded measurements, translating simple fluid velocities and loss rates to shear stress functions. The average erosion rate δm at given velocity v is obtained using equation (2), where m (kg) is the amount of soil eroded during a selected time interval δt (sec) for each velocity; d (m) is the diameter of the soil sample exposed to the flood erosion test. The shear stress is obtained using equation (3), where τ is the shear stress on the wall of the pipe; f is the friction factor obtained from the Moody diagram depending on the Reynolds number R and pipe roughness ε/D ; ρ is the mass density of water (1,000 kg/m³); and v is the mean flow velocity of pipe. As the MEFA has a rectangular cross section pipe, D is taken as the hydraulic diameter; D = 4 A/P where A is cross-sectional flow

area; P is wetted perimeter; and the factor 4 is used to ensure that the hydraulic diameter is equal to the equivalent diameter of a circular pipe.

$$\delta m = \frac{4m}{\delta t \pi d^2} \tag{2}$$

$$\tau = \frac{1}{8} f \rho v^2 \tag{3}$$

For a partially filled rectangular pipe, hydraulic diameter of the rectangular cross section pipe is determined with equation (4), where a and b are the dimensions of the sides of the rectangle. As the pipe is partially filled, the wetted perimeter consists of the three sides of the duct that is two on the side (a) and the base (b). Figure 1 shows the erosion apparatus in action with a burned soil specimen at the beginning of the erosion testing process.

$$D = \frac{4ab}{(2a+b)} \tag{4}$$

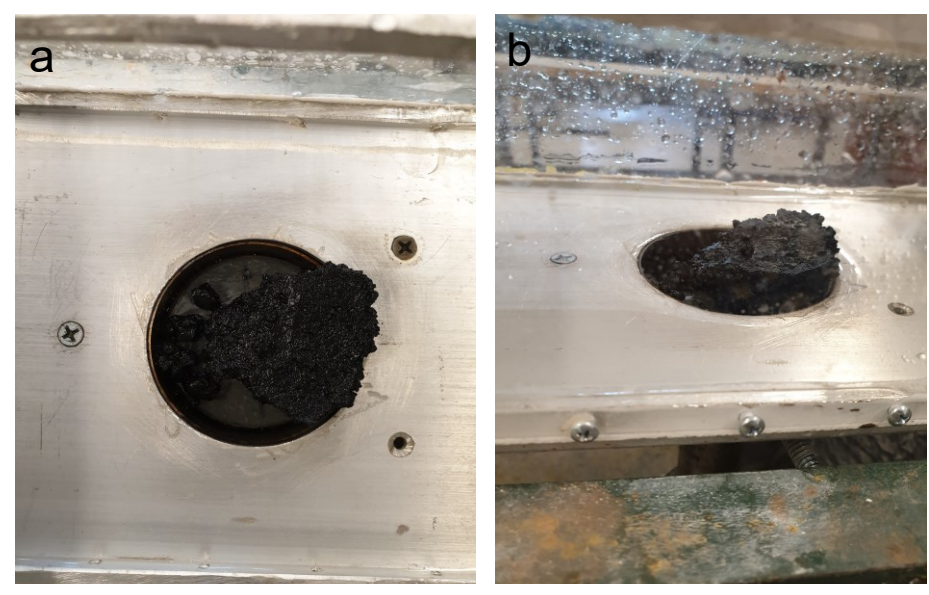


Figure 1. Image of an erosion test through the sidewall of the test device. A single large piece of burned soil breaking away in the test device under high velocity rather than more gradual erosion. This sample was molded at 25% water content at an initial dry density of 1.52 g/cm³ and thus has a more compact texture and blocky erosion mechanism.

2. Experimental Studies

2.1 Material Properties and Sample Preparation

The soil used in this pilot testing program was a composite of material sampled from the B1 and B2 (refer to Table 2) soil horizons that was remolded at controlled moisture contents and dry densities. The same mineral composition as that sampled in the B1 and B2 layers dominated soil horizons A, E, and C. Depth to which weathered rock structure could be identified varied from 0.5 to 2m. Parent rock consisted of red shales and limestones. Mica is frequently present in the local shales, and mica is present in the soils sampled at an approximate rate of 3 to 6% by weight

per X-ray diffraction analysis. Other soils in the Black Hills can have mica contents of up to 60% by weight and in the dry summers are locally known as "moon dust." These soils were avoided for this sampling program, as high mica contents are not typical to the Western US. The soil chemistry is both alkaline and saline, with high amounts of chlorides, sulfates, and pH of 8 to 9.

Table 1 presents the soil characterization information for the sampled soil used in the erosion testing program, while Table 2 presents the typical lithology by comparing dry unit weight and organic content. Table 1 does not include isolated gravels and cobbles in the soil but focuses on the soil matrix around the larger clasts. As seasonal fluctuations in soil water content are continuous and influenced heavily by localized vegetation type and sun exposure, water contents for each layer are not reported. However, water contents at the time of sampling in the late spring of 2020 were typically 15 to 25% by weight, at to moist of optimum. The soil material is red to red-brown to brown depending on soil horizon and water content. The duff and tree litter above the soil varied in thickness of 2 cm to 8 cm and consisted mostly of pine needles, small twigs, pinecones and dead grasses. Surface vegetation was typically small evergreen conifer shrubs and a thinly distributed mixture of native and non-native annual and perennial grasses and clovers.

Table 1: Summary of laboratory test results and physical properties of soil used in erosion tests

Properties	Measured Values	ASTM Test Designation	
USCS	SC	D2487	
Course Fraction (%)	74 to 84	D422	
Fine Fraction (%)	16 to 26	D422	
Clay Fraction (%)	6 to 11	D422	
D ₅₀ (mm)	0.2 to 0.5	D422	
Specific Gravity, Gs	2.7	D854	
Liquid Limit, LL (%)	30 to 34	D4318	
Plastic Limit, PL (%)	17 to 20	D4318	
Plasticity Index, PI (%)	13 to 14	D4318	
Shrinkage Limit (%)	6 to 7	D4318	
OMC (%)	13 to 16	D698	
Max dry density (kN/m³)	19.2 to 19.4	D698	

Soil samples were remolded after initial sampling, air drying, and moisture conditioning to known densities and water contents. This allowed for a parametric flexibility in trying to better understand the wildland fire soil erosion phenomena. Specimens were remolded using moist tamping into steel rings using three thin lifts. Specimens were 25.4-mm high cylinders of 63.5-mm diameter. Once prepared, specimens were wrapped in plastic to prevent moisture loss in the time between remolding and the wildfire simulation burn. The wildfire simulation burn was performed by placing a steel pan in a shallow pit dug into the earth. The steel pan allows for control of specimen material loss from the rings out of the bottom of the rings. A thin layer of silica sand was prepared at the bottom of the pan to that rings did not sit on steel. Rings were placed at the center of the pan and clean silica sand was used to surround all rings and fill any annuluses between rings. Thermistors were installed atop specimens, below specimens, and below the pan at several locations to monitor temperatures. A 6-cm layer of duff from the sampling site was then placed on the soil. Overtop of the duff, pine branches and logs were placed for fuel and the fire was lit.

Table 2: Summary of native soil lithology

Soil Horizon	Dry Density (kN/m3)	Organics (% by Weight)
A1 (roots but little humus)	14.4 to 14.6	6 to 12
A2 (humus)	14.4 to 14.6	5 to 9
A3 (lowest grass roots)	15.0 to 16.2	2 to 4
E (significant mineral leaching)	15.2 to 16.8	1 to 3
B1 (lowest shrub roots; few gravels)	17.4 to 18.3	1 to 3
B2 (lowest lateral tree roots; isolated cobbles)	17.4 to 18.3	<1
C (many gravels and cobbles)	18.7 to 19.2	<1

The wildland fire simulation is carried out by monitoring the temperatures at the top of the soil, below the duff, and at the bottom of the rings and pan so that realistic temperatures appropriate of an intense and severe wildfire with burning logs was attained. Rather than simulating grass fire or crown fire, higher temperatures in the soil are found via either smoldering fire or when logs burn. Once the fire reached a soil surface temperature of 800C, the fire was held constant at 800C soil surface temperature for 75 minutes, after which burning fuel is removed and any fuels smoldering are allowed to cool naturally for 24-hours before removal of specimens from the simulator. The experimental setup allowed for consistent temperatures in the rings and a consistent atmosphere around the rings for a consistent time in each burn event to prepare specimens. Once specimens are removed from the wildland fire simulation burning pit, they are carefully brushed to remove the ash layer, any remaining cinders, and unburned vegetative litter of the duff (if any). Brushing is continued until the burned mineral soil is approximately 1mm below the top of ash. This removal of ash and other debris is done so that soil erosion can be studied here. We note that in field erosion studies, that the sediment load of the ash and debris layer is a critical component of degraded stream quality. However, our purpose is to study to soil erosion potential in this paper.

2.2 Erosion Function Apparatus

Erodibility of soil is associated with the erosion rate and the hydraulic shear stress (τ) (Briaud et al., 1999). Several laboratory tests set up have been developed in the past to evaluate the erosion potential of fine-grained soils. Moore and Masch Jr (1962) proposed rotating cylinder apparatus for evaluating the erosion potential of fine-grained cohesive soil. Rohan et al. (1986) proposed a drill hole apparatus to improve the rotating cylinder test to evaluate the erosion of cohesive soils. This drill hole apparatus is similar to the pinhole test equipment and Moody diagram has been used to find out the friction factor of the eroded surface. Briaud et al. (2001) developed Erosion Function Apparatus (EFA) to evaluate the relationship between the soil erosion rate and water velocity or interfacial shear stress.

Previous Erosion Function Apparatus (EFA), constructed by Briaud in 2001, had rectangular pipe of 101.6 X 50.8 mm cross section area and was 1.22 m long. The Shelby tube with a 76.2 mm outside diameter was used to observe the bed erosion behavior of soil sample. In this study, a modified Erosion Function Apparatus (MEFA) is developed to observe erosion potential of fine-grained plastic soil and the schematic diagram of this experimental setup is shown in Figure 2. This test set consists of a 1.27 m long rectangular pipe with a cross section area of 177.8 mm X 140 mm. A pump with valve is fixed to circulate and regulate the rate of flow of water with a mean velocity range of 0.5-5 m/s. A circular hole with 62 mm outer diameter is provided on the bottom side of the rectangular pipe to accommodate the Shelby tube samplers. During the test, one end of the Shelby tube with soil sample is placed fastened with the bottom of a rectangular pipe. A hydraulic jack is placed at the bottom end of the sampling Shelby tube that pushes the soil until it exposes 1 mm into the rectangular pipe and get exposed to water flow. A watertight connection is stablished at the joint of Shelby tube and rectangular pipe.

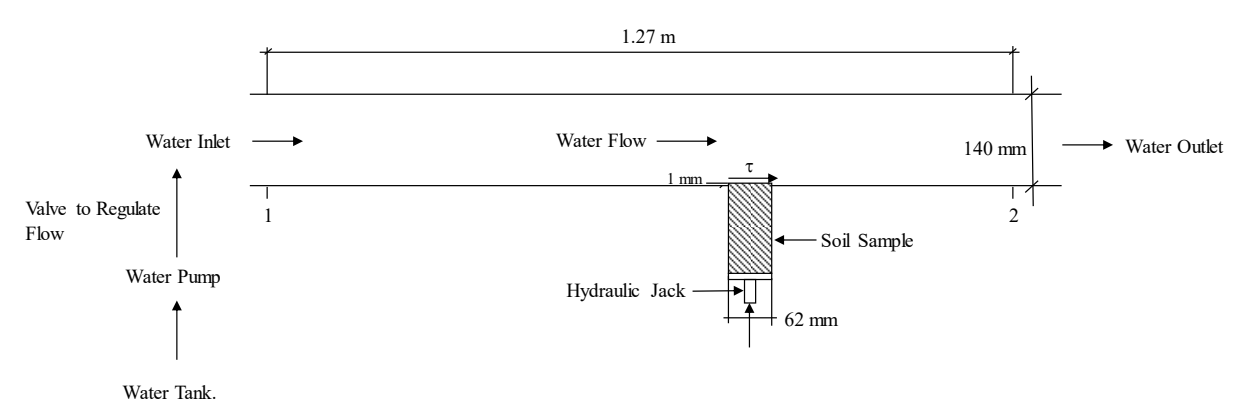


Figure 2. Schematic diagram of MEFA

In this study, control unburned soil and burned soil were prepared in multiple "trials" that represent distinct burn events. The soils were remolded to varying initial dry densities (1.12 to 1.52 g/cm³) with three water contents of 5%, 15%, and 25%. These water contents represent near optimum, with variations of 10% on the wet and dry sides of optimum. The dry densities were selected based on field observations of the different horizons. The range is indicative of different soil histories that can be present at a single site, with some areas being compacted more by human activity, while other areas loosened by successive millennia of flora and fauna. Erosion tests were carried out on the samples using the MEFA device.

Within the device, the experiment proceeds as follows. At first, the uppermost 1 mm of the soil sample is exposed to the water flow at 0.1 m/s for until the 1 mm soil is eroded. The time taken for the 1 mm soil erosion was recorded and the velocity was increased from 0.1 m/s to 0.7 m/s to record the time taken for eroding a new 1 mm soil sample. Same procedure is followed up to 5 m/s for different velocities. Sediment loss for untreated and treated samples were measured for each test run after each velocity. For each flow velocity, erosion rate (kg/s/m²) is achieved by dividing the sediment loss by the area of the soil sample and the time required to do so.

3. Results and Discussion

3.1 Relation of Erosion Rate with Velocity and Shear Stress

Erosion test results for two trials (i.e. burn events) with three different dry densities of the soil are shown in Figure 3, where higher densities resulted in less erosion, generally, except at the highest fluid velocity. In the case of the highest fluid velocity, the 1.44 g/cm³ specimens experienced higher erosion than the less dense counterparts. This was due to the 1.44 g/cm³ specimens having a different texture after burning. In these specimens, the soil experienced slightly more vitrification of clay particles and creating of more calcite than the less dense specimens and as a result had more distinct aggregations after the burn events. It is unknown why these two specimens had more vitrification and calcining. Localized higher temperatures in the simulated wildfire burn event are the suspected cause. However, the general trend in the testing program is that the less dense the soil, the greater the erodibility, the two specimens in Figure 3 excepted.

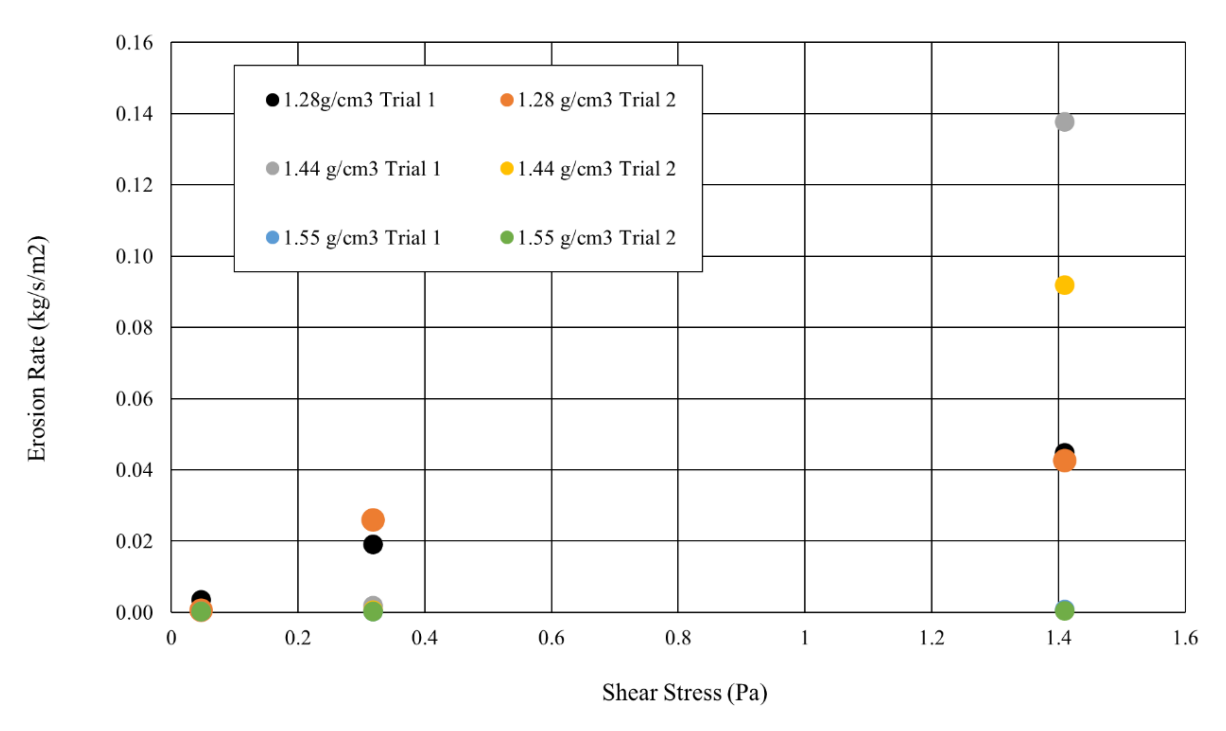


Figure 3. Erosion test results for burned soils at varying initial remolded dry densities at constant water content (15%).

Examination of every specimen after burning and during erosion testing showed that two observable phenomena supplement the hydrophobicity phenomena in changing post-fire soil erodibility. In forthcoming publications, we show that in specimens that are initially at higher initial water contents burn hotter than the lower water content specimens. The vaporization of water is proposed as the key mechanism to this difference. In these higher water content specimens, slight vitrification of clay particles is observed, as is slightly more calcining. Calcining is a temperature-initiated process in which calcite is created. Thus, specimens at higher water contents are more resistant to erosion. Figure 4 presents the erosion trends from a single initial dry density (1.12 g/cm³) at varying initial water contents. We also note that remolding at optimum water content or wet of optimum creates a more flocculated soil structure, and that this flocculated structure also aids in resisting erosion. Between the denser structure and the

additional strengthening and hydrophobicity, it is clear that initial water content is a critical metric for understanding this post-fire erosion behavior.

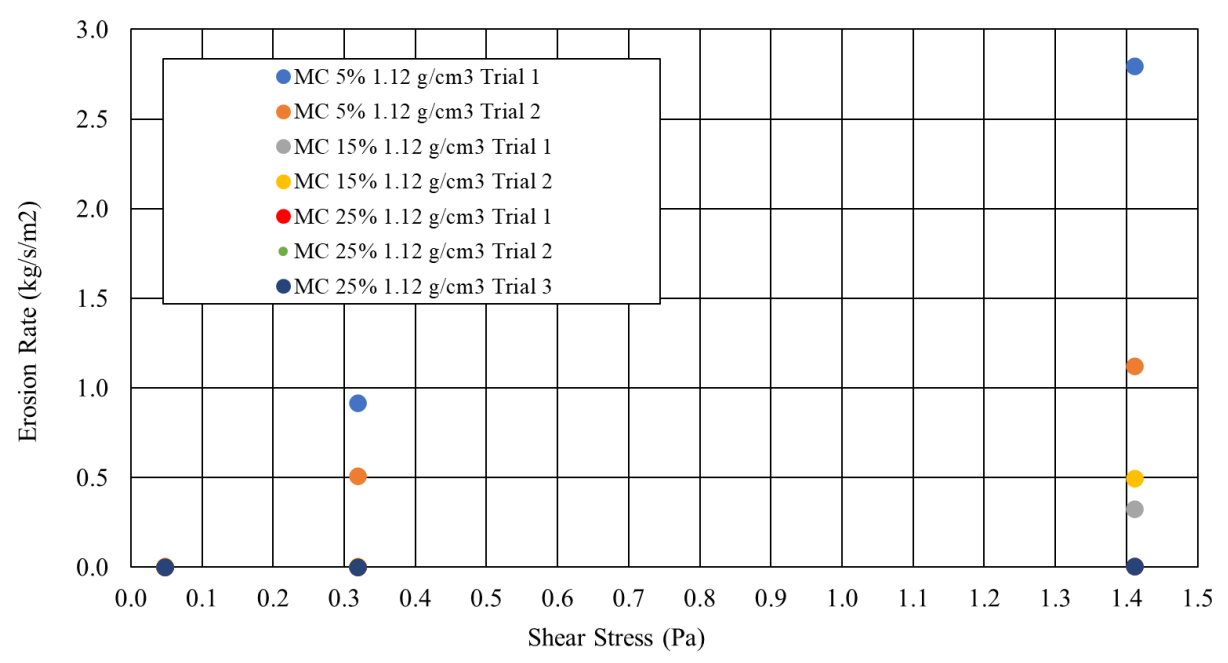


Figure 4. Erosion test results for burned soils for a constant low remolded density at varying water contents.

Lastly, Figure 5 compares a set of unburned control specimens to their burned analogs. The comparison of unburned controls to the wildfire specimens is that the unburned specimens experience more erosion and have higher erodibility than their burned counterparts. This is most pronounced at lower density and at lowest water contents. Hydrophobicity was not measured in this research, although it was observed visually. This is an area of needed continued research. These results show that although density has the greatest effect on erosion potential, the secondary effects of vitrification of clay particles, calcining, and hydrophobicity align to reduce the erosion potential in soils after intense and sever wildland fire (assuming no ash is present).

4. Conclusions

Following a wildland fire simulation of burning, soil specimens of a clayey sand from the Black Hills of South Dakota and Wyoming in the United States were tested for erosion susceptibility. In the experiments, conventional trends of erodibility held for the burned soil: decreasing density resulted in greater erosivity, while compaction at or wet of optimum moisture decreased erosivity. Soils with water contents below the optimum water content eroded at a higher rate than would be expected after burning. At higher densities, no noticeable differences were observed between burned and unburned specimens. However, at lower densities soils that were burned exhibited less erosivity that their unburned counterparts. The unburned control specimens at lower densities eroded at higher rates than the burned specimens. This is due to two observed phenomena. First, the burned soils developed slight hydrophobicity. Second, the burned soil clay content was

partially vitrified and weak calcite was formed at the soil surface. Although the ash and debris layers were removed from these specimens so that the soil itself could be observed, these findings indicate that following intense and severe wildland fire, that soil erosion potential of the Bhorizons if exposed, is less than that of surrounding unburned soils similarly exposed (i.e. the dozer lines). These results also show that soil erosion after a fire is most sensitive to the water content at the time of burning, and that greater soil moisture results in less erodibility, as higher water content soils have elevated temperatures that result in additional vitrification of clay and creation of more calcite, while generating more hydrophobicity.

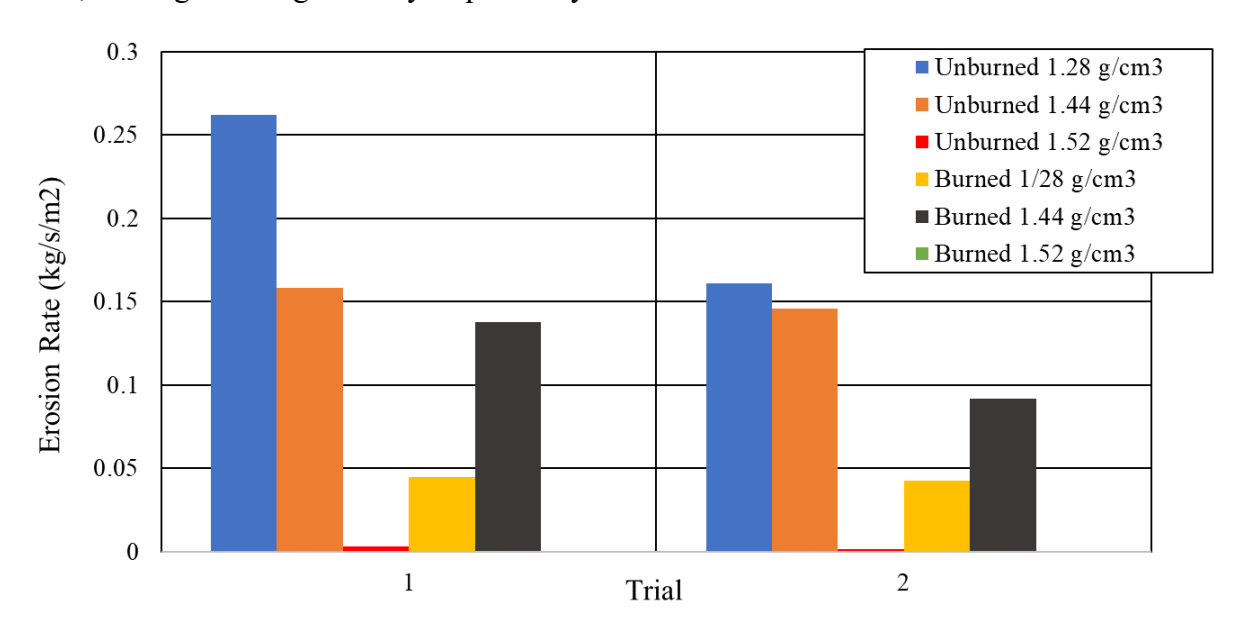


Figure 5. Differences in erosion rates from burned versus unburned soils remolded at the same initial dry densities and water content (15%) at fluid velocity of 0.7 m/s (shear stress of 1.41 Pa). The highest density specimens had less than 1mm loss after 1-hour.

References:

Al-Durrah, M., and Bradford, J. (1982). "The mechanism of raindrop splash on soil surfaces 1". *Soil Science Society of America Journal*, 46(5), 1086-1090.

Bonilla, C. A., and Johnson, O. I. (2012). "Soil erodibility mapping and its correlation with soil properties in Central Chile". *Geoderma*, 189, 116-123.

Briaud, J.-L., Ting, F., Chen, H., Cao, Y., Han, S., and Kwak, K. (2001). "Erosion function apparatus for scour rate predictions". *Journal of Geotechnical and Geoenvironmental Engineering*, 127(2), 105-113.

Briaud, J.-L., Ting, F. C., Chen, H., Gudavalli, R., Perugu, S., and Wei, G. (1999). "SRICOS: Prediction of scour rate in cohesive soils at bridge piers". *Journal of Geotechnical and Geoenvironmental Engineering*, 125(4), 237-246.

Bryan, R. B. (2000). "Soil erodibility and processes of water erosion on hillslope". *Geomorphology*, 32(3-4), 385-415.

DeBano, L.F. 2000a. Water repellency in soils: a historical overview. *Journal of Hydrology*. 231-232: 4–32.

DeBano, L.F. 2000b. The role of fire and soil heating on water repellency in wildland environments: a review. *Journal of Hydrology*. 231-232: 195–206.

- Doerr, S.H.; Shakesby, R.A.; Walsh, R.P.D. 2000. Soil water repellency: its causes, characteristics and hydro-geomorphological signifigance. *Earth Science Reviews*. 51(1-4): 33–65.
- Dong-Sheng, Y., Xue-Zheng, S., and Weindorf, D. (2006). "Relationships between permeability and erodibility of cultivated Acrisols and Cambisols in subtropical China". *Pedosphere*, 16(3), 304-311.
- Grissinger, E. H. (1966). "Resistance of selected clay systems to erosion by water". *Water resources research*, 2(1), 131-138.
- Le Bissonnais, Y., Renaux, B., and Delouche, H. (1995). "Interactions between soil properties and moisture content in crust formation, runoff and interrill erosion from tilled loess soils". *Catena*, 25(1-4), 33-46.
- Moore, W. L., and Masch Jr, F. D. (1962). "Experiments on the scour resistance of cohesive sediments". *Journal of Geophysical Research*, 67(4), 1437-1446.
- Robichaud, PR. 2000. Fire and erosion: evaluating the effectiveness of a post-fire rehabilitation treatment, contour-felled logs. In: *Proceedings, watershed management and operations management conference*; 2000 June 20–24; Fort Collins, CO. Reston, VA: American Society of Civil Engineers. 11 p.
- Robichaud, P.R. 2002. Wildfire and erosion: when to expect the unexpected. *Symposium on the geomorphic impacts of wildfire*. Paper 143-10. Boulder, CO: Geolological Society of America. 1 p.
- Robichaud, P.R.; Brown, R.E. 1999. What happened after the smoke cleared: onsite erosion rates after a wildfire in eastern Oregon. In: *Olsen, D.S.; Potyondy, J.P. (eds.). Proceedings, wildland hydrology conference*; 1999 June; Bozeman, MT. Hernon, VA: American Water Resource Association: 419–426.
- Robichaud, P.R.; Hungerford, R. 2000a. Water repellency by laboratory burning of four northern Rocky Mountain forest soils. *Journal of Hydrology*. 231–232: 207–219.
- Robichaud, P.R.; Beyers, J.L.; Neary. D.G. 2000b. Evaluating the effectiveness of postfire rehabilitation treatments. Gen. Tech. Rep. RMRS-GTR-63. Fort Collins, CO: U.S. Department of Agriculture, Forest Service, Rocky Mountain Research Station. 85 p.
- Rohan, K., Lefebvre, G., Douville, S., and Milette, J.-P. (1986). "A new technique to evaluate erosivity of cohesive material". *Geotechnical Testing Journal*, 9(2), 87-92.
- Shaikh, A., Ruff, J. F., Charlie, W. A., and Abt, S. R. (1988). "Erosion rate of dispersive and nondispersive clays". *Journal of Geotechnical Engineering*, 114(5), 589-600.
- Sharif, Y. A., Elkholy, M., Hanif Chaudhry, M., and Imran, J. (2015). "Experimental study on the piping erosion process in earthen embankments". *Journal of Hydraulic Engineering*, 141(7), 04015012.
- Shields, A. (1936). "Anwendung der Aehnlichkeitsmechanik und der Turbulenzforschung auf die Geschiebebewegung". *PhD Thesis Technical University Berlin*.
- Singh, H. V., and Thompson, A. M. (2016). "Effect of antecedent soil moisture content on soil critical shear stress in agricultural watersheds". *Geoderma*, 262, 165-173.
- Wischmeier, W. H., and Mannering, J. (1969). "Relation of soil properties to its erodibility". *Soil Science Society of America Journal*, 33(1), 131-137.